COMPUTATIONAL SIMULATION OF ELECTRIC FIELDS SURROUNDING POWER TRANSMISSION AND DISTRIBUTION LINES

J. Patrick Donohoe*
Min-Yee Jiang**
Joe F. Thompson**
David B. Miller*

*Department of Electrical and Computer Engineering
Mississippi State University
P.O. Drawer EE
Mississippi State, MS 39762

**Engineering Research Center for Computational Field Simulation
Mississippi State University/National Science Foundation
P.O. Box 6176
Mississippi State, MS 39762

ABSTRACT

A numerical technique is presented for computing the potential distributions surrounding power transmission and distribution lines of complex geometry. The technique employs a finite difference solution using boundary-fitted coordinates. A newly developed finite difference solver code is coupled with the existing EAGLE grid generation code to yield a system capable of solving for the electric potential and field distributions surrounding complex configurations. A code validation example is presented which consists of a sphere-to-ground electrostatic solution. Sample results are also presented for a distribution line model.

INTRODUCTION

The voltage level at which a power transmission or distribution line fails (the critical flashover voltage) is dependent on the physical configuration of the line under test. The cross-sectional geometries of lines in use today vary widely given various supporting structures, insulators and conductors. The critical flashover voltage of a newly-designed configuration is commonly determined through construction and experimental testing. In some cases, attempts at reproducing experimental results fail because the arc traverses different paths to ground from test to test. In the design of transmission and distribution lines, prediction of the failure point is often accomplished by comparing the new configuration to a geometrically similar configuration which has previously been tested. A more effective method of predicting the failure point of a given configuration is to determine the potential and field distribution through computational means. This technique would greatly enhance the design of high voltage transmission and distribution lines by providing the designer a tool to investigate changes in the insulation properties of a given line due to minor design modifications without expensive experimental tests. An accurate plot of the potential and field distributions surrounding the line would yield insight into the maximum allowable voltage levels and the phenomenon of multiple paths to ground from failure to failure.

Computation of the electric potential distribution throughout some arbitrarily shaped two-dimensional or three-dimensional region involves the numerical solution of the governing partial differential equation. Since high voltage transmission and distribution lines carry either direct current or low frequency (60 Hz) alternating current signals, the potential distribution for breakdown calculations may be determined assuming no time variation. Under static conditions, the potential distribution is governed by either Poisson's or Laplace's equation, depending on the distribution of free electric charge in the region of interest [1]. The periodic placement of supporting structures along the length of any transmission or distribution line makes the problem of modelling such a configuration inherently three-dimensional.

The representation of the surface boundary conditions is a critical factor in the accuracy of the final solution to a given partial differential equation. The accurate numerical representation of surface boundary conditions for a transmission or distribution line with a complex supporting structure is by no means trivial. A particularly effective technique of accurately describing boundary conditions on an arbitrarily shaped body is through boundary fitted coordinates (numerical grid generation) [2], [3], [4]. A curvilinear coordinate system is defined in the region of interest such that all boundaries in the region are coincident with coordinate lines. The coordinate system describing the physical region is then transformed into a fixed rectangular computational field defined by a square mesh. The resulting system of finite difference equations in the transformed or computational space consists of simply described boundary conditions. The equations to be solved in the computational space are more complex than those in the original physical space, but the accuracy of the solution is enhanced through the precise representation of the surface boundary conditions in the computational space. The finite difference solutions to the equations in the computational space are obtained using only grid points so that no interpolation between grid points is required. The grid point placement is dictated by the field variation in the region of interest. Grid points are concentrated in regions where the field variation is rapid while widely-spaced grid points are used in regions where the field is near-constant.

The electric potential distributions computed in this research were obtained using a newly developed solver code coupled with the existing EAGLE grid generation code [5] to yield a system capable of solving for potential distributions surrounding transmission and distribution line configurations defined by complex geometries. The grid system in the region surrounding the transmission line model of interest is constructed using the EAGLE code. The finite difference method is utilized to solve the governing partial differential equation over the domain of interest subject to the appropriate boundary conditions.

FORMULATION

Given some static distribution of electric charge, the resulting electric scalar potential (V) may be determined as a function of position by solving the appropriate boundary value problem. The differential equation which describes the potential distribution in a region of (free) electric charge is Poisson's equation given by

$$\nabla^2 V = -\frac{\rho}{\varepsilon} \tag{1}$$

where ∇^2 is the Laplacian operator, ρ is the electric charge density (C/m^3) and ε is the permittivity (F/m) of the medium. In a region where no free charge is present, Poisson's equation reduces to Laplace's equation:

$$\nabla^2 V = 0 \quad . \tag{2}$$

The solutions to Poisson's and Laplace's equations are obtained by enforcing the appropriate boundary conditions to the general solution of the respective differential equation. These boundary conditions may be expressed in terms of the scalar electric potential, the vector electric field $\boldsymbol{E}$ (V/m) or the vector electric flux density $\boldsymbol{D}$ (C/m^2). The static electric field is defined in terms of the electric scalar potential by

$$\boldsymbol{E} = -\nabla V \tag{3}$$

where ∇ is the gradient operator. Thus, boundary conditions described in terms of the vector electric field may be related to the electric scalar potential using Equation (3). The general equations which describe the behavior of the electric field and flux across a surface discontinuity are well known [1,6,7] and are given by

$$\hat{\boldsymbol{n}} \times \left[\boldsymbol{E}_2 - \boldsymbol{E}_1 \right] = 0 \tag{4}$$

and

$$\hat{\boldsymbol{n}} \cdot \left[\boldsymbol{D}_2 - \boldsymbol{D}_1 \right] = \rho_S \tag{5}$$

where $(\boldsymbol{E}_1, \boldsymbol{D}_1)$ are vector quantities in region 1, $(\boldsymbol{E}_2, \boldsymbol{D}_2)$ are vector quantities in region 2, and $\hat{\boldsymbol{n}}$ is a unit normal to the surface which points into region 1. The vector electric flux density is related to the vector electric field by

$$\boldsymbol{D} = \varepsilon \boldsymbol{E} \quad . \tag{6}$$

The boundary conditions in Equations (4) and (5) can be related to the scalar potential using Equations (3) and (6) which yields

$$\hat{\boldsymbol{n}} \times \left[(\nabla V)_1 - (\nabla V)_2 \right] = 0 \tag{7}$$

and

$$\hat{\boldsymbol{n}} \cdot \left[\varepsilon_1 (\nabla V)_1 - \varepsilon_2 (\nabla V)_2 \right] = \rho_S \quad . \tag{8}$$

Equations (7) and (8) represent the general boundary conditions for the scalar potential across a surface discontinuity.

In cases where an isolated conductor is located in an applied electric field, the resulting conductor potential is unknown ("floating" conductor). When a conductor is placed in a static electric field, a charge distribution is induced on the conductor surface which produces a zero-valued electric field everywhere inside the conductor yielding a constant-valued potential throughout the conductor. The total surface charge on the conductor remains unchanged given any applied electric field distribution. From Gauss' Law, the integral of the normal component of the electric flux density over the outer surface of the charged conductor (S) yields the total charge on the conductor such that

$$\int_S \boldsymbol{D} \cdot d\boldsymbol{s} = Q \tag{9}$$

where the direction of $d\boldsymbol{s}$ is an outward pointing normal ($d\boldsymbol{s} = \hat{\boldsymbol{n}}\, ds$), ds defines the differential surface element on the conductor surface and Q is the initial value of total charge on the conductor. The integral defined in Equation (9) may be expressed in terms of potential by relating the electric flux density to the potential which yields

$$\int_S \varepsilon \left[\hat{\boldsymbol{n}} \cdot (\nabla V) \right] ds = -Q \tag{10}$$

where the dielectric surrounding the conductor is assumed to be isotropic.

Assuming the transmission or distribution line model is composed of perfect conductors and lossless dielectrics, the regions of interest with regard to potential and field computations (external to the conductors and throughout the dielectrics) are charge-free. Thus, a solution to Laplace's equation is required. Given a curvilinear coordinate system defined by (ξ^1, ξ^2, ξ^3), the Laplacian operator in non-conservative form [2] is given by

$$\nabla^2 V = \sum_{i=1}^{3} \sum_{j=1}^{3} g^{ij} V_{\xi^i \xi^j} + \sum_{k=1}^{3} (\nabla^2 \xi^k) V_{\xi^k} \tag{11}$$

where the subscripts on V denote partial derivatives and g^{ij} is the contravariant metric tensor. The elements of the contravariant metric tensor are defined as dot products of the contravariant unit vectors (normals to the curvilinear coordinate surfaces denoted by $\hat{a}^i$) which yields

$$g^{ij} = \hat{a}^i \cdot \hat{a}^j \quad . \tag{12}$$

The Laplacian term in Equation (11) may be written as

$$\nabla^2 \xi^k = g^{kk} P_k \tag{13}$$

where P_k is a control function evaluated in the course of the grid generation and is then available to the Laplace solver as coefficients with fixed values at each grid point. Laplace's equation can now be written as

$$\sum_{i=1}^{3}\sum_{j=1}^{3} g^{ij} V_{\xi^i \xi^j} + \sum_{k=1}^{3} g^{kk} P_k V_{\xi^k} = 0 \quad . \tag{14}$$

The first and second order derivatives found in Equation (14) are represented by central difference approximations and the overall equation is solved using the successive over-relaxation (SOR) iterative technique.

Four basic boundary conditions on the scalar potential are required in the formulation of the numerical model: the Dirichlet boundary condition, the Neumann boundary condition, the material interface boundary condition and the floating conductor boundary condition. The Dirichlet boundary condition is characterized by a scalar potential which is constant on a particular boundary. The surface of all conductors are defined as Dirichlet boundaries since they represent equipotential volumes. The application of the Dirichlet boundary condition is trivial using boundary-fitted coordinates. Scalar potential values are fixed at grid points on the specified surface (ξ^i=constant) and these values are preserved throughout the iterative process.

The Neumann boundary condition is defined by a zero-valued normal derivative of the potential on a given boundary. The Neumann boundary condition is applied at the outer boundaries of the volume enclosing the transmission line model. The normal derivative to the coordinate surface on which ξ^i is constant is given by

$$V_n^i \doteq \frac{\partial V}{\partial n} = \frac{1}{\sqrt{g^{ii}}} \sum_{j=1}^{3} g^{ij} V_{\xi^j} \tag{15}$$

which yields

$$\sum_{j=1}^{3} g^{ij} V_{\xi^j} \qquad (\xi^i = constant) \tag{16}$$

as the Neumann boundary condition on the given surface.

A floating conductor is an equipotential volume but the conductor potential is an unknown value. Thus, the initial charge condition defined in Equation (10) must be coupled with the Dirichlet boundary condition for a floating conductor. Such a boundary condition can be enforced by integrating the normal component of electric flux over the conductor surface or over some surface enclosing the conductor. Both methods of integration produce similar results but the structure of the corresponding grids are totally different. Integrating over a surface enclosing the conductor allows for a multi-block grid with a smaller number of blocks than integrating over the conductor surface. The advantage of using a small block system is to obtain better control of the grid distribution in the regions of interest and to reduce the I/O overhead needed to transfer iterative data from block to block.

The material interface boundary conditions are applied at dielectric-dielectric interfaces and conductor-dielectric interfaces. The tangential electric field boundary condition of Equation (7) is implicit in the formulation since the scalar potential is assumed to be continuous across the boundary. The normal electric flux boundary condition of Equation (8) on the coordinate surface where ξ^i is constant may be stated as

$$\frac{\varepsilon_1}{\sqrt{g^{ii}}} \sum_{j=1}^{3} g^{ij} V_{\xi^j} - \frac{\varepsilon_2}{\sqrt{k^{ii}}} \sum_{j=1}^{3} k^{ij} V_{\xi^j} = \rho_s \tag{17}$$

where g^{ij} and k^{ij} are the contravariant metric tensors evaluated on the grid at the interface in region 1 and region 2, respectively.

COMPOSITE-BLOCK GRID STRUCTURE

The curvilinear coordinate system mentioned in the previous section is constructed using the EAGLE grid generation code. The EAGLE code is a composite (multi-block) algebraic or elliptic grid generation system designed to discretize the domain in and around any arbitrary shaped three-dimensional region. The concept of the composite-block structure is described in detail in [5].

Fundamental to the curvilinear coordinate system is the coincidence of some coordinate surface with each boundary of the physical region. The physical region of interest in divided into contiguous subregions (interfacing hexahedrons), and each subregion can be transformed to a rectangular block in the computational space, with a grid generated within each subregion. Each subregion has its own curvilinear coordinate system irrespective of that in the adjacent subregions. Each subregion, defined by six generally curved sides, is transformed to a rectangular computational region on which the curvilinear coordinates are the independent variables. In principle, it is possible to establish a correspondence between any physical region and a rectangular block in the computational space, but the resulting grid may be too skewed for a complicated geometry. In such a case, the given physical region must be subdivided into smaller blocks until the resulting grid satisfies the user-defined grid criterion with regard to skewing.

The general curved surfaces bounding the sub-regions in the physical space form internal interfaces across which information must be transferred. In the computational space, the information must be transferred from the side of a given rectangular block to the corresponding side of the adjacent block. These two sides of the adjacent blocks correspond to the same physical surface. The interface is treated as a branch cut on which the function value is solved just as it is in the interior of the blocks. The interfaces of the blocks are not fixed, but are determined by the solver. The most straightforward technique to employ is to provide an extra layer of points surrounding each block. These surrounding points represent points across the given interface just inside the adjacent block. This relationship is maintained throughout the iterative procedure. The governing partial differential equation is solved by point SOR iteration using a field of locally optimum acceleration parameters. These optimum parameters make the solution robust and capable of convergence with strong control functions.

CODE VALIDATION EXAMPLE

An analytically solvable electrostatic problem is attempted in order to validate the code. The problem considered here is that of a conducting sphere over ground. The sphere over ground problem is solved numerically and compared with the equivalent problem of two isolated conducting spheres. For the two sphere problem, the electric field along the line connecting the sphere centers may be expressed as an infinite series using images as given in [8]. This problem has similar characteristics to the power distribution line problem in that one is interested primarily in the electric field and potential in the region between the conductors while these quantities are less critical away from this region. Also, the outer

boundary of the sphere-to-ground problem has the same general characteristics of the transmission/distribution line problem with a ground plane on the floor of the region and the remainder of the outer boundary on which the potential is unknown.

The geometry of the sphere-to-ground problem is shown in Figure 1 where D is the sphere diameter, S is the spacing between the sphere surface and the ground plane, and B is the dimension of the cubical outer boundary. The particular geometry chosen is D=100cm, S=50cm and B=20D. Note that the x coordinate origin is located at the sphere center and extends downward to the ground plane. Thus, the domain of interest for field comparison purposes is $50\text{cm} \leq x \leq 100\text{cm}$. A three block, h-type grid is generated in the given volume of interest with a total of 88,263 grid points. Comparisons of the computed electric field with analytic results are shown in Figures 2 and 3 using two distinct outer boundary conditions. A constant potential of V=0 is assumed on the ground plane and on all outer boundaries for the first boundary condition (Figure 2). For the second boundary condition (Figure 3), the ground plane potential is again assumed to be V=0 but the Neumann boundary condition is enforced on the other outer boundaries. In both cases, excellent agreement is found between the analytic and computed results.

The uniform V=0 outer boundary condition described above is viable for problems involving conductors of limited extent in all three dimensions such as the sphere-to-ground problem. However, for problems involving conductors which span the entire spatial domain in one or more dimension, such as a transmission or distribution line model, the constant outer boundary condition is inadequate and the Neumann boundary condition may be applied. The Neumann boundary condition, which forces the computed equipotential contours to lie normal to the outer boundary, yields appropriate behavior in the vicinity of the ground plane where the equipotential contours "follow" the ground plane. Negligible errors in the electric field are experienced in the regions of interest by choosing the outer boundaries sufficiently far away as shown in the sphere-to-ground example.

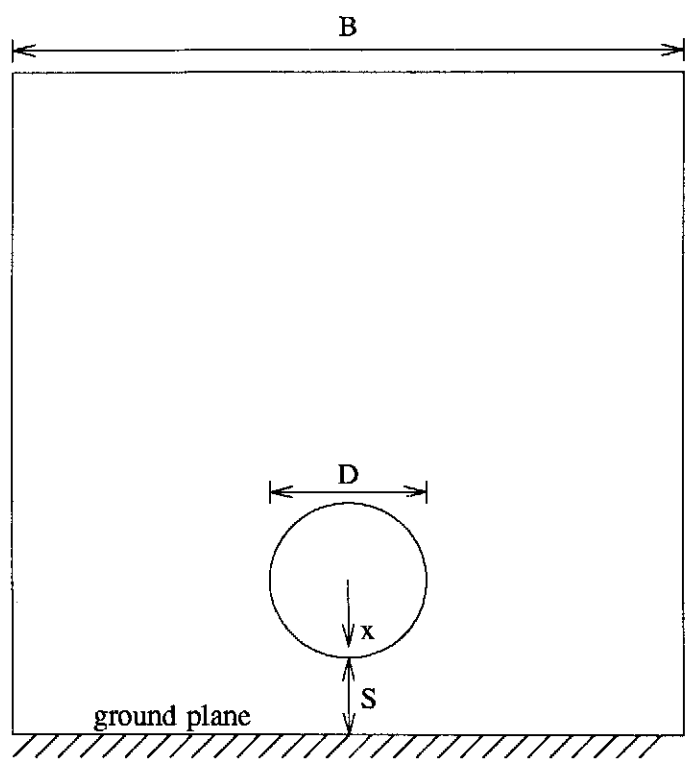

Figure 1. Sphere-to-ground geometry.

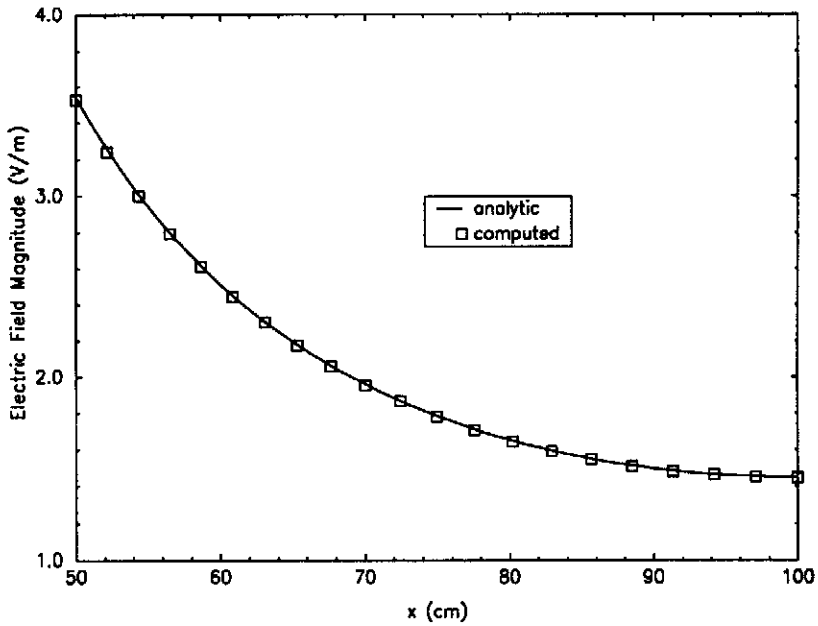

Figure 2. Comparison of the analytical sphere-to-ground electric field with computed results given V=0 on all outer boundaries.

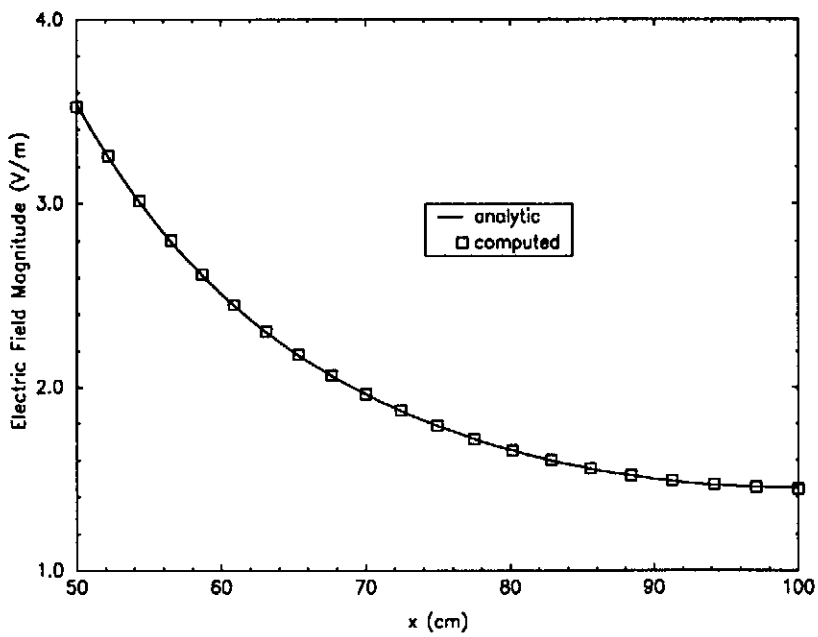

Figure 3. Comparison of the analytical sphere-to-ground electric field with computed results using the Neumann boundary condition on all outer boundaries excluding the ground plane.

POWER DISTRIBUTION LINE MODEL

The critical flashover voltage of a typical distribution line configuration was studied experimentally by Jacob, et. al. in [9]. The distribution line model shown in Figure 4 is a simplified version of the experimental configuration analyzed in the aforementioned study. Insulators, crossarm braces and

mounting hardware components have been omitted in the distribution line model to simplify the geometry of the resulting grid. A detailed description of the distribution line numerical model is given in Table 1. Conductors A, B and C represent the three high-voltage conductors (phases) while conductor N is the neutral wire and conductor G is the vertical ground wire.

Several configurations of charged, floating and grounded phases were studied experimentally in [9]. A single phase was charged in order to measure the critical flashover voltage of the phase-to-ground and phase-to-phase failures. Two of the models considered in [9] are analyzed here and designated as model #1 and model #2. For model #1, the B phase is charged with the A and C phases floating. For model #2, the B phase is charged while the A phase is grounded and the C phase is floating. The ground plane, conductor N and conductor G are held at 0 volts for both models. The potential of the charged conductor is assumed to be 1 volt for both models.

The volume enclosing the three-dimensional distribution line model is defined by ($-400" \leq x \leq 200"$), ($0" \leq y \leq 1200"$) and ($-90" \leq z \leq 90"$) with the axis of the pole located along the y-axis. A four-block grid system is constructed with the grid points distributed throughout the volume as illustrated in Figure 5. Note that the grid points are concentrated in the region of interest surrounding the conductors in the vicinity of the pole. A total of 96,525 grid points were used to determine the three-dimensional potential distributions: 75 in the x-direction, 39 in the y-direction and 33 in the z-direction. The computed potential distributions are plotted over surfaces defined by k=constant where k is the grid point index in the z-direction (k=0 defines the plane where z=−90", k=33 defines the plane where z=90"). Due to the grid structure, the surfaces defined by k=constant are not planar in the vicinity of the pole as shown in Figure 6.

RESULTS

The potential distributions are computed for both model #1 and model #2 given the charged conductor (phase B) is charged to 1 volt. The resulting potential distributions are plotted over constant k surfaces in the vicinity of the charged conductor. The potential distributions surrounding model #1 for k=1, k=17 and k=19 are shown in Figures 7, 8 and 9, respectively. The corresponding potential distributions surrounding model #2 for k=1, k=17 and k=19 are shown in Figures 10, 11 and 12, respectively. The potential difference between the equipotential contours is 0.02 volts.

The initial "guess" for the potential values has a significant effect on the number of iterations required for a prescribed accuracy. The first results were obtained by assuming a zero-valued potential at all grid points as the starting values. A significant reduction in the run time was obtained for both three-dimensional models by utilizing the corresponding two-dimensional results as the initial values on the surfaces normal to the axes of the wires. The two-dimensional results are those associated with the same distribution line minus the pole, crossarm and vertical ground wire. As expected, the potential distribution of the three-dimensional model approaches that of the two-dimensional model as one moves away from the supporting structure.

Several physical effects associated with discrete components of the numerical model have been noted for the configurations which were analyzed. The effect on the potential distribution of a floating conductor of small cross-sectional dimension is found to be minimal. Conversely, a floating conductor can alter the potential distribution considerably if the conductor cross-section is of significant physical dimension. The floating conductor represents an equipotential volume (surface) so that the resulting equipotential contours in the surrounding medium must wrap around the conductor. The equipotential contours on the end faces of the volume enclosing the three-dimensional model over perfect ground are predominantly horizontal below the charged conductors since the contours must "follow" the ground plane (equipotential surface). The effect of a vertical ground wire located on the supporting structure is to pull the equipotential contours upward as one moves from the end face toward the supporting structure such that the equipotential contours wrap around the ground wire. A large electric field is generated in the vicinity of the ground wire as the equipotential contours crowd together. The effect of the wood pole is

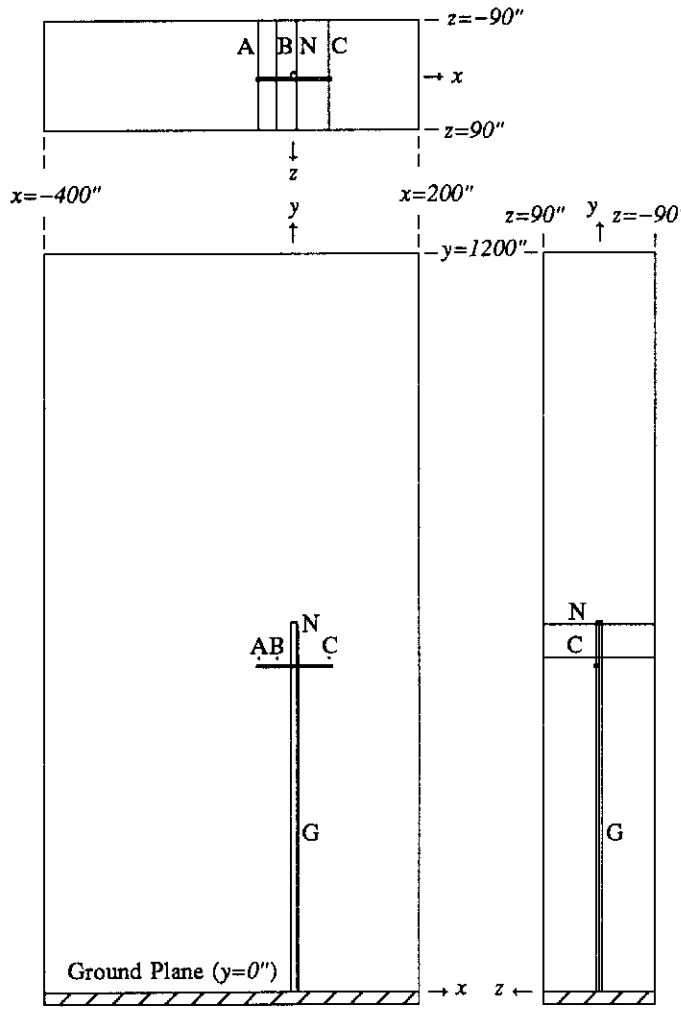

Figure 4. Three-dimensional distribution line model.
(See Table 1 for detailed description.)

Enclosing Volume - [$-400" \le x \le 200"$, $0" \le y \le 1200"$, $-90" \le z \le 90"$]
Ground Plane - Perfectly conducting ground plane (x-z plane)
Pole - Southern pine ($\varepsilon=3.5\varepsilon_o$) 50 ft. pole, *10"* diameter, axis of the pole lies along the y axis
Crossarm - Southern pine ($\varepsilon=3.5\varepsilon_o$) 10 ft. crossarm, *120"x4.5"x5"*, centerline of crossarm is 44 ft. above the ground plane
Conductors - Each conductor is modelled as a filament, A Phase - wire axis located at $x=-56"$, $y=541.25"$ B Phase - wire axis located at $x=-27"$, $y=541.25"$ C Phase - wire axis located at $x=56"$, $y=541.25"$ Neutral (N) - wire axis located at $x=5"$, $y=595"$ Ground wire (G) - wire axis located at $x=5"$, $z=0"$

Table 1. Description of the distribution line model.

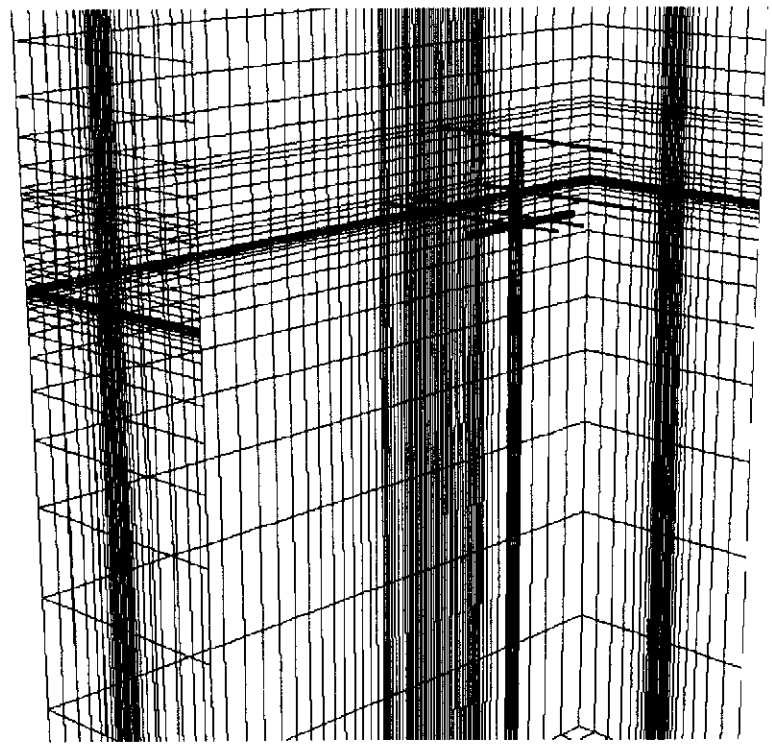

Figure 5. Three-Dimensional Distribution Line Model Grid.

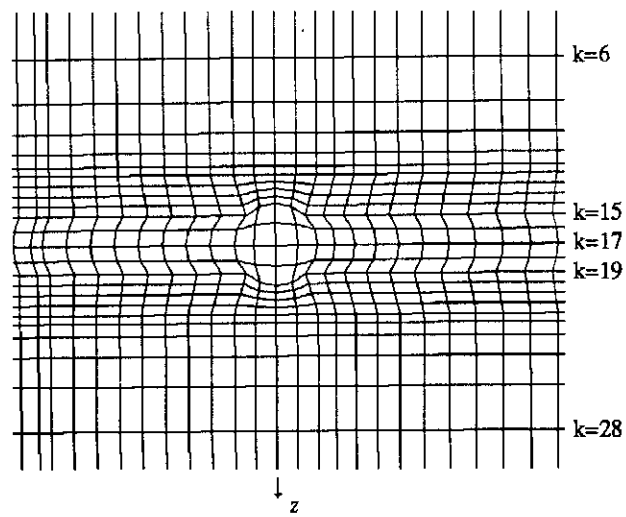

Figure 6. Cross-Sectional Contours in the Vicinity of the Pole.

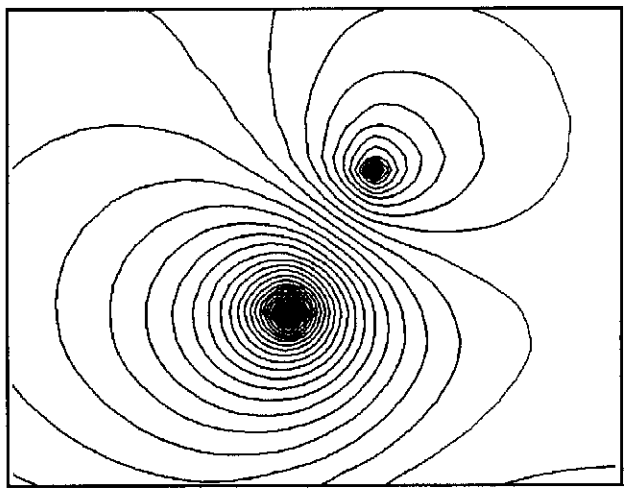

Figure 7. Model #1 Potential Distribution (k=1).

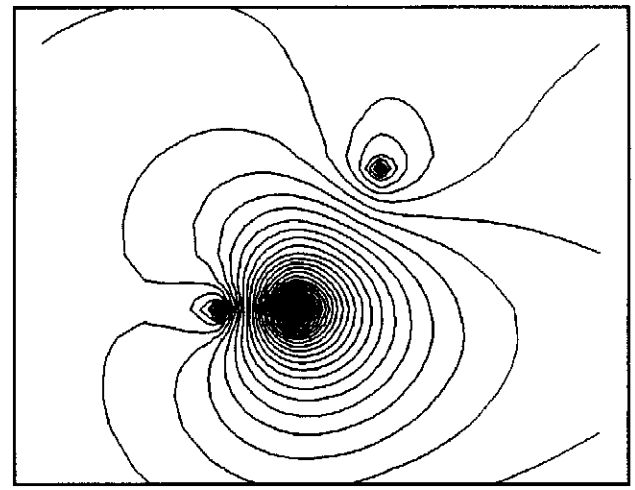

Figure 10. Model #2 Potential Distribution (k=1).

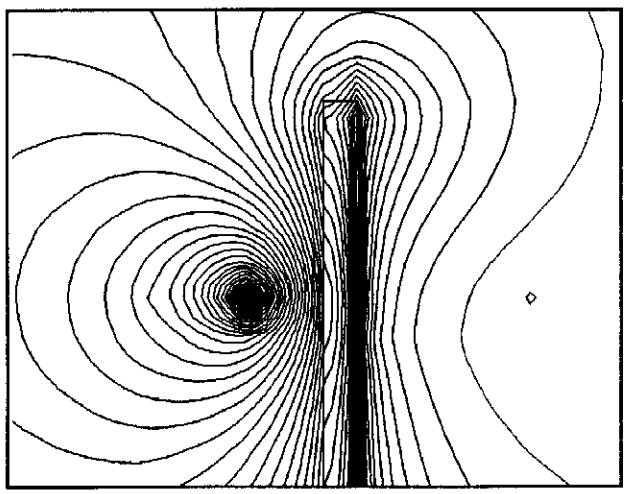

Figure 8. Model #1 Potential Distribution (k=17).

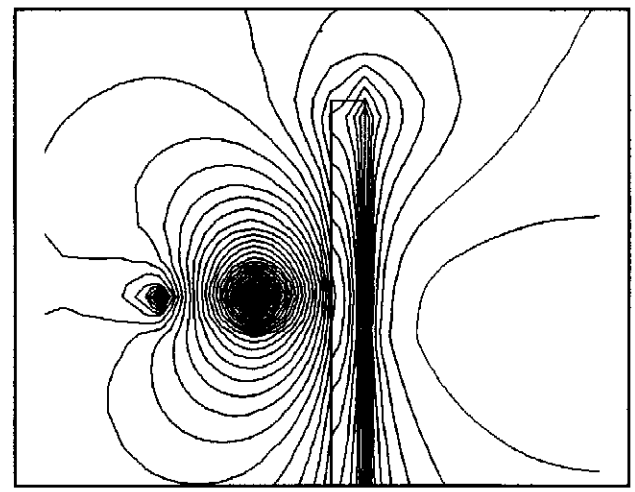

Figure 11. Model #2 Potential Distribution (k=17).

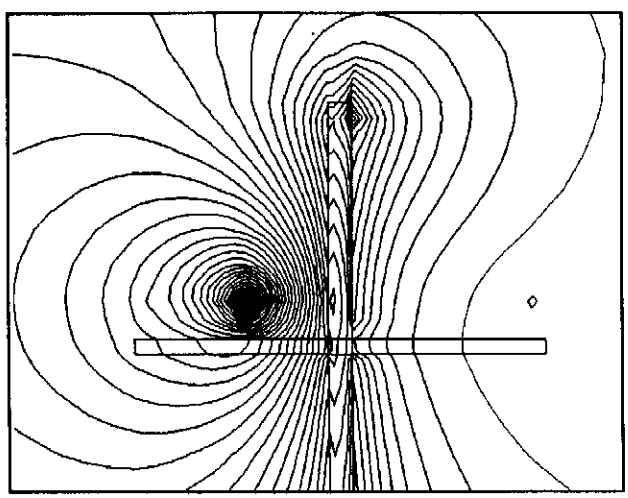

Figure 9. Model #1 Potential Distribution (k=19).

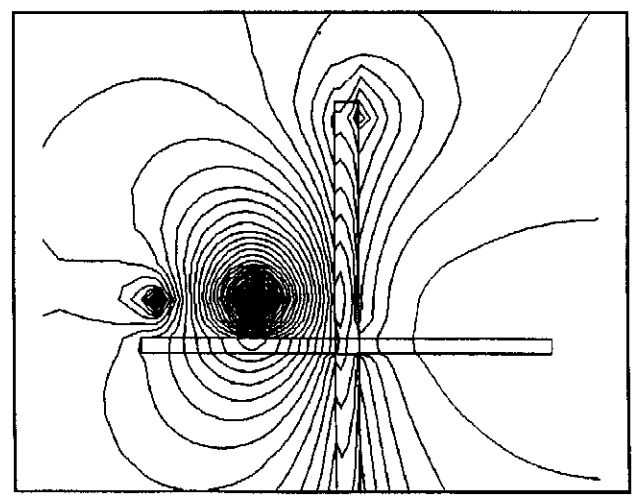

Figure 12. Model #2 Potential Distribution (k=19).

to reduce the electric field as one moves from the surrounding air into the wood. This reduction in the electric field is caused by the bending of the equipotential contours away from the air-wood interface inside the wood region.

A more realistic model of the distribution line studied in [9] must include the insulators and associated mounting hardware. Of particular interest is the metal bolt on which the insulator is mounted. This bolt would be modelled as a perfect conductor and thus represent a floating conductor of significant cross-sectional dimension. This floating conductor would be located in close proximity to a charged conductor. The resulting equipotential contours surrounding the bolt would crowd around the equipotential volume creating a large electric field. In such a manner, the effect of the bolt would be to alter the flashover path. The present research forms the basis for further work in which the physics of the air breakdown process are incorporated into the code in an attempt to actually predict the critical flashover voltage using a computational model.

CONCLUSIONS

The potential distributions surrounding a three-dimensional distribution line model has been computed by solving Laplace's equation throughout the enclosing volume. The partial differential equation solution was carried out using a newly developed solver code coupled with an existing grid generation (EAGLE) code. The code allows for a system model which consists of charged and/or floating conductors along with multiple dielectrics. Given a three-dimensional transmission or distribution line model, using the corresponding two-dimensional solution (the solution for the transmission line without the supporting structure) as the initial value on each cross-section of the enclosing volume enhances the convergence properties of the solution significantly. The actual potential distribution on the end faces of the enclosing volume are found to be quite similar to the corresponding two-dimensional solution.

REFERENCES

[1] J. D. Kraus, *Electromagnetics*, Third Edition, McGraw-Hill, 1984, pp. 63-68.

[2] J. F. Thompson, Z. U. A. Warsi and C. W. Mastin, *Numerical Grid Generation: Foundations and Applications*, North-Holland, 1985.

[3] J. F. Thompson, F. C. Thames, and C. W. Mastin, "Automatic Numerical Generation of Body-Fitted Curvilinear Coordinate System for Field Containing Any Number of Arbitrary Two-Dimensional Bodies", *J. Comp. Phys.*, Vol. 15, No. 3, July 1974, pp. 299-319.

[4] J. F. Thompson, "A Composite Grid Generation Code for General 3-D Regions", American Institute of Aeronautics and Astronautics 25th Aerospace Sciences Meeting, January, 1987, Reno, Nevada.

[5] J. F. Thompson, "Program EAGLE - User's Manual, Vol. 1,2,3," USAF Armament Laboratory Technical Report AFATL-TR-88-117, Eglin AFB, Florida, 1988.

[6] J. A. Stratton, *Electromagnetic Theory*, McGraw-Hill, 1941, pp. 163-165.

[7] R. F. Harrington, *Time Harmonic Electromagnetic Fields*, McGraw-Hill, 1961, p.34.

[8] E. Kuffel and W. S. Zaengl, *High-Voltage Engineering*, Pergamon Press, 1984, p. 224-228.

[9] P. B. Jacob, S. Grzybowski and E. R. Ross, "A Guide to Estimating Lightning Insulation Levels of Overhead Distribution Lines", Mississippi State University Final Report to the Electric Power Research Institute, RP 2874-01, May 1989.

ACKNOWLEDGEMENT

Partial support for this research was provided by the Electric Power Research Institute under Research Project RP2871-1, Task 6. The remaining support was provided by the Research Center for Advanced Scientific Computing at Mississippi State University. Through funding from the National Science Foundation, the Research Center for Advanced Scientific Computing has evolved into the Engineering Research Center for Computational Field Simulation.